JOURNAL OF MATERIALS SCIENCE 31 (1996) 3839–3845

On the influence of the chromium content on the evolution of rolling textures in ferritic stainless steels

D. RAABE
Institut für Metallkunde und Metallphysik, RWTH Aachen, Kopernikusstr. 14, 52056 Aachen, Germany

The crystallographic hot and cold rolling textures of various ferritic stainless steels with 10.5–16.5 wt % Cr content were investigated by use of quantitative texture analysis. The hot-rolled specimens revealed a texture gradient through the sheet thickness. In the centre layers they revealed a cold-rolling type texture (α-fibre) and close to the surface layers a strong Goss orientation. The texture maximum as well as the through-thickness texture gradient of the hot-rolled specimens increased with the Cr content. During cold rolling the textures inherited from the hot rolling process sharpened in the centre layers and decreased in the sub-surface layers. The hot band textures from which this inhomogeneity proceeded were explained in terms of the strong through-thickness profile of the shear strains. The fact that the textures were not randomized by phase transformation during hot rolling was attributed to the elevated Cr content which stabilizes the ferritic regime.

1. Introduction

Due to their good mechanical properties and corrosion resistance ferritic stainless steels represent an important group of construction materials for numerous technical applications. The mechanical behaviour of polycrystalline materials is considerably affected by the orientation distribution of the crystallites which is referred to as crystallographic texture. The determination of the texture is of great technical importance since by accounting for the anisotropic behaviour of each unit cell it defines the directional properties of the polycrystal [1, 2]. In the case of ferritic stainless steels texture research has gained considerable importance in optimizing the deep drawing properties and avoiding the ridging phenomenon which often deteriorates the surface of such alloys.

The evolution of the orientation distribution of ferritic stainless steels with 10.5–16.5 wt % chromium (Cr) content during hot and cold rolling has been the subject of various studies in the past employing either two-dimensional pole figure projections [3, 4] or the three-dimensional orientation distribution function (ODF) [5–14].

Whereas the underlying slip mechanisms which lead to the formation of the rolling textures are quite well understood in terms of relaxed constraints Taylor type simulations [8, 9, 13–17] the influence of the Cr content on the texture evolution has not yet been clarified adequately. The present study is hence primarily concerned with the investigation of the influence of the Cr content on the formation of the hot and cold rolling textures of ferritic stainless steels.

2. Experimental details

Sixteen ferritic stainless steels containing 10.5–16.5 wt % Cr and 0.01–0.02 wt % C were investigated. Some of the data presented were extracted from previous works [5–9, 18–21]. All steels were industrially manufactured by continuous casting and subsequent unidirectional hot rolling, passing 7 four high stands for rolling, to a final thickness of 3–3.5 mm. The first pass was carried out within the temperature range, 1400 to 1460 K and the last one within the range, 1200 to 1300 K. After hot rolling the steels were annealed at 1300 K.

Cold rolling was carried out on a laboratory rolling mill to a final deformation of $\varepsilon_{11} = 90\,\%$. The samples were rotated 180° about the transverse direction after each pass. Since homogeneous deformation is primarily determined by the ratio of contact length, l_d, to sheet thickness, d, a ratio of $1 < (l_d/d) < 3$ was obtained during cold rolling.

All textures were quantitatively examined by measuring the four incomplete pole figures {1 1 0}, {2 0 0}, {1 1 2}, and {1 0 3} in the back reflection mode [22]. The measurements were conducted in the range of the pole distance angle α from 5 to 85° using MoK_{α_1} radiation. Since the interpretation of pole figures taken from polycrystals is ambiguous because of the superposition of the same poles from different orientations, the orientation distribution function (ODF) was computed by use of a conventional Fourier type series expansion method [1, 2]. In the case of cubic crystal symmetry and orthorhombic sample symmetry (rolling direction RD, normal direction ND and transverse

0022–2461 © *1996 Chapman & Hall*

direction TD) an orientation can then be presented by the use of three Euler angles φ_1, ϕ and φ_2 in the reduced Euler space ($0° \leq \varphi_1 \leq 90°$, $0° \leq \phi \leq 90°$, $0° \leq \varphi_2 \leq 90°$).

Since body centred cubic (b c c) metals tend to develop very symmetric textures (e.g. [23–28]) it is convenient to describe the orientation distributions observed in terms of texture fibres, which can either be presented using iso-intensity plots (φ_1-sections) or the so called fibre diagrams [9, 14, 23, 24]. Frequently employed texture fibres are the α-fibre, which contains all orientations $\{hkl\}$ $\langle 1\,1\,0\rangle$, the γ-fibre, which comprises all orientations $\{1\,1\,1\}$ $\langle uvw\rangle$, the η-fibre containing all components $\{hkl\}$ $\langle 0\,0\,1\rangle$ and the ε-fibre which includes all orientations with a crystal $\langle 1\,1\,0\rangle$ axis parallel to TD (Fig. 1).

As has been frequently documented, the texture and microstructure of ferritic stainless steels is very inhomogeneous through the sheet thickness [5–9]. All samples were thus measured in at least two different through-thickness layers. Some specimens were investigated even in eleven succeeding layers. The layer under investigation is described by the parameter s, which indicates the distance between layer and sample centre divided by the half thickness ($s = 0$ centre, $s = 1$ surface). In the present study usually the centre layer ($s = 0$) and the sub-surface layer ($s = 0.8$) were investigated. From previous studies it is well established [5–9] that most of the relevant texture components are located in these layers. In order to remove a layer of 20×10^{-6} m prior to the texture measurement the samples were etched in a solution of 50 ml H_2O_2 and 10 ml HF.

3. Results

3.1. Hot rolling

In Fig. 2 the texture of a hot-rolled sample with 16.5 wt % Cr content is presented by use of fibre diagrams. This sample which reveals the main features characteristic of hot band textures of ferritic stainless steels was investigated in eleven different layers. In the centre layer a strong α-fibre which is dominated by the $\{0\,0\,1\}$ $\langle 1\,1\,0\rangle$ and $\{1\,1\,2\}$ $\langle 1\,1\,0\rangle$ texture components (Fig. 2a), accompanied by a weak γ-fibre is developed (Fig. 2b). Close to the surface layer a very strong $\{0\,1\,1\}$ $\langle 1\,0\,0\rangle$ component, which is referred to as Goss orientation (Fig. 2c), and a very weak α-fibre are generated (Fig. 2a). Plotting the orientation density of a typical texture component as a function of the hot band layer provides a suitable tool for describing the through-thickness texture gradient.

In Fig. 3 a typical profile of the Goss orientation through the thickness of three ferritic stainless steels containing 16.5 wt % Cr is shown. From this presentation it is evident that close to the surface layers ($s = 0.8$) a strong maximum of the Goss component occurs whereas in the centre layers ($s = 0$) it does not appear at all. Steels with 10.5 wt % Cr content essentially show the same type of texture profile through the sheet thickness. However, the maximum orientation density frequently occurring at $\{0\,0\,1\}$ $\langle 1\,1\,0\rangle$, $\{1\,1\,2\}$ $\langle 1\,1\,0\rangle$ and Goss is usually somewhat lower compared to steels containing 16.5 wt % Cr [19]. The inhomogeneity of the hot band texture is also well known from other ferritic stainless steels [e.g. 5–14] and Fe 3 wt % Si transformer steels (e.g. [25, 29]) provided that they are not entirely hot rolled in the austenitic region.

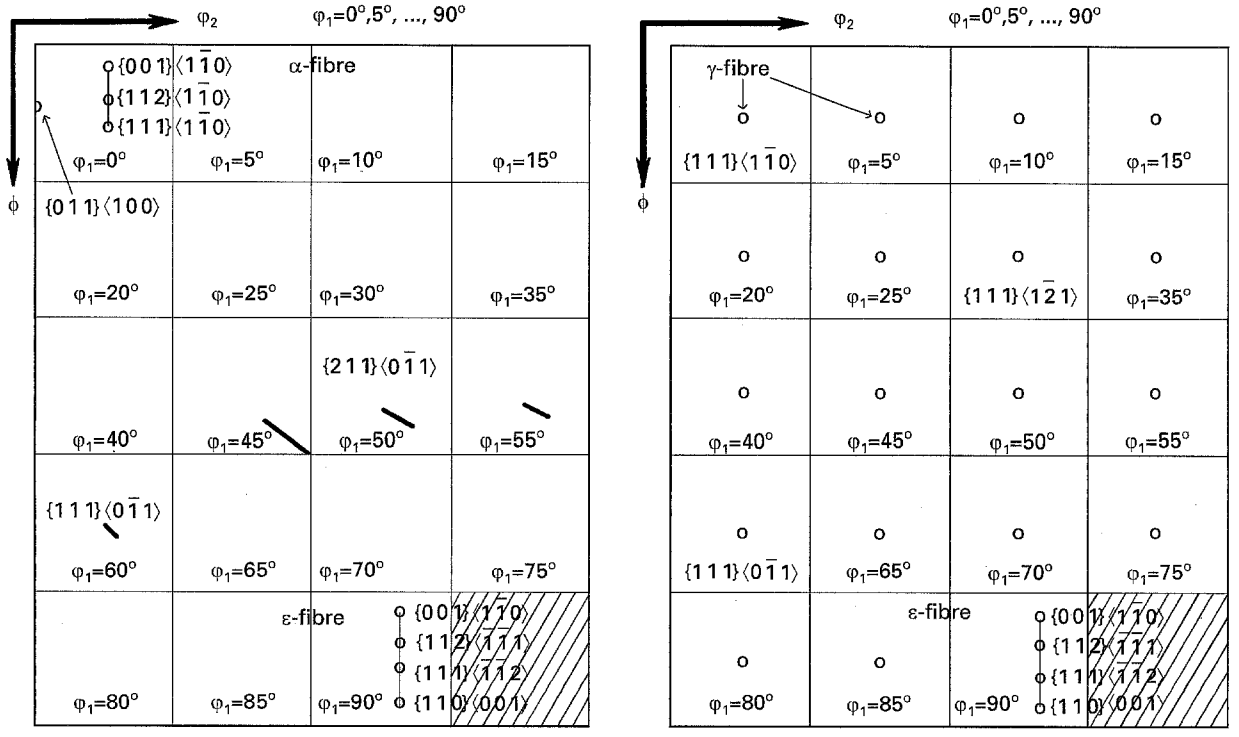

Figure 1 Euler space with some important b c c texture fibres and orientations, φ_1-sections.

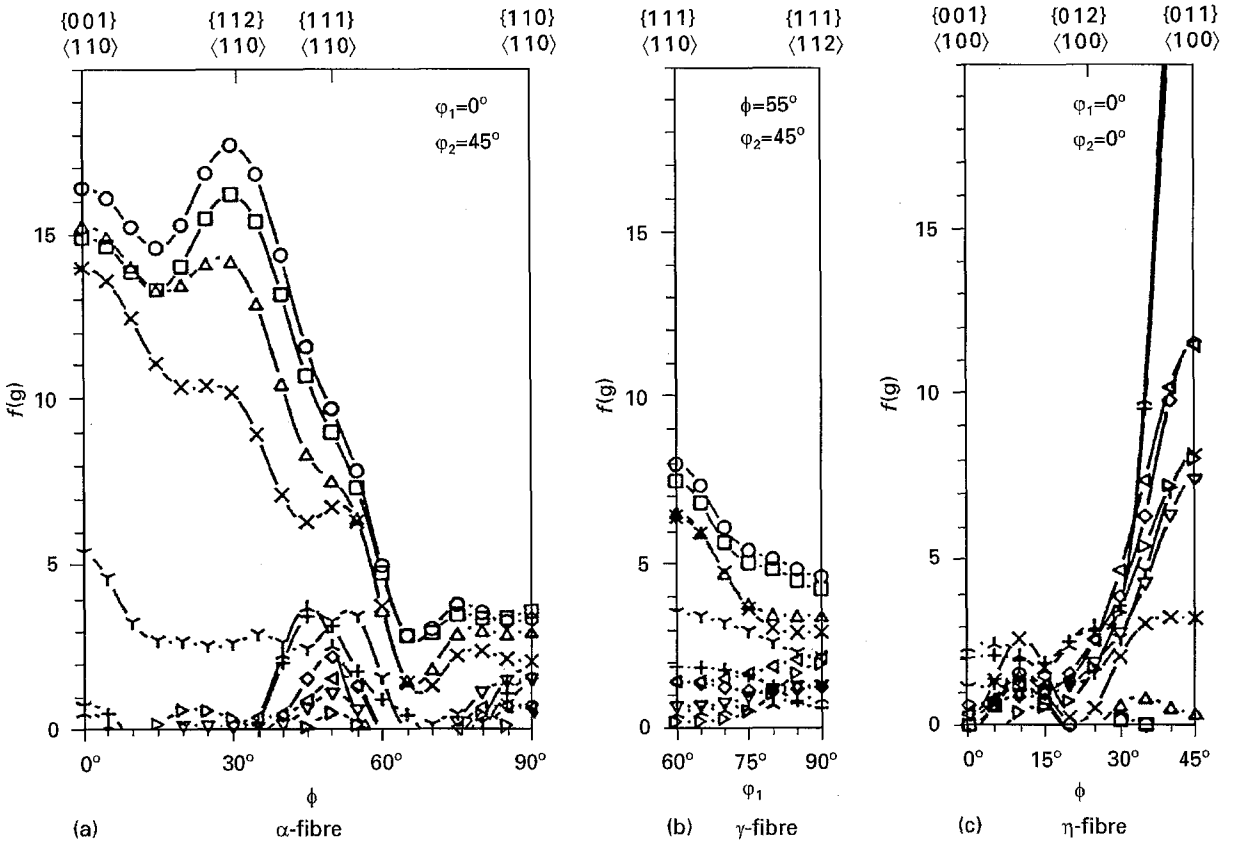

Figure 2 Hot rolling texture of Fe–16.5 wt % Cr in fibre presentation. Through-thickness texture profile: (a) α-fibre, (b) γ-fibre, and (c) η-fibre. Key: ○ $s = 0.0$ (centre); □ $s = 0.1$; △ $s = 0.2$; × $s = 0.3$; ⌒ $s = 0.4$; ◇ $s = 0.5$; ▽ $s = 0.6$; + $s = 0.7$; ⌒ $s = 0.8$; ▷ $s = 0.9$; ◁ $s = 1.0$ (surface).

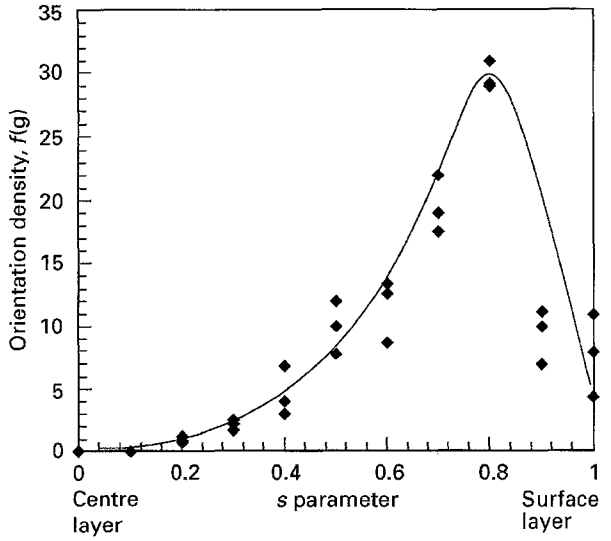

Figure 3 Profile of the Goss orientation through the thickness of three different ferritic stainless steels containing 16.5 wt % Cr. The occurrence of the Goss texture indicates strong shear deformation. Key: ◆ Goss component.

3.2. Cold rolling

Owing to the inhomogeneous hot band textures the steels under investigation also reveal a very inhomogeneous evolution of their corresponding cold rolling textures. A typical example is shown for a steel with 10.5 wt % Cr content (Figs 4 and 5), which reveals the same type of texture profile through the sheet thickness as steels containing 16.5 wt % Cr (Figs 2 and 3). Whereas in the centre layer ($s = 0$) a strong texture with a maximum orientation density at {0 0 1} ⟨1 1 0⟩ is revealed (Fig. 4a) close to the surface ($s = 0.8$) Goss prevails (Fig. 5c).

After $\varepsilon_{11} = 50\%$ in the centre layer a strong α-fibre texture ranging from {0 0 1} ⟨1 1 0⟩ to {1 1 1} ⟨1 1 0⟩ accompanied by a weak {1 1 1} ⟨1 1 2⟩ component has developed (Fig. 4a). This texture is entirely inherited from the hot band and has been sharpened slightly during subsequent cold rolling. The texture on the ε-fibre remains nearly unchanged during cold rolling (Fig. 4c). In contrast, in the sub-surface layer, a considerable texture transition takes place (Fig. 5). Since grains with an initial Goss orientation (Fig. 5c) are no longer stable under the plane strain conditions imposed during cold rolling they rotate either towards {0 0 1}⟨1 1 0⟩ (α-fibre) or {1 1 1} ⟨1 1 2⟩ (γ-fibre) [8, 13].

As is shown in Fig. 4a, after a deformation of $\varepsilon_{11} = 60\%$ in the centre layer the α-fibre is increased. In the sub-surface layer the Goss component is completely degraded and a weak α-fibre texture, mainly consisting of a pronounced {0 0 1} ⟨1 1 0⟩ orientation, is developed (Fig. 5a and c). Both the {0 0 1} ⟨1 1 0⟩ and the {1 1 1} ⟨1 1 2⟩ components, the orientation density of which is much higher than in the centre layer (Figs 4b and 5b), are essentially generated by previously Goss oriented crystals [8, 13, 14]. After $\varepsilon_{11} = 70\%$ the α-fibre texture is even more pronounced (Fig. 4a). In the sub-surface layer (Fig. 5) the {0 0 1} ⟨1 1 0⟩ orientation on the α-fibre still appears

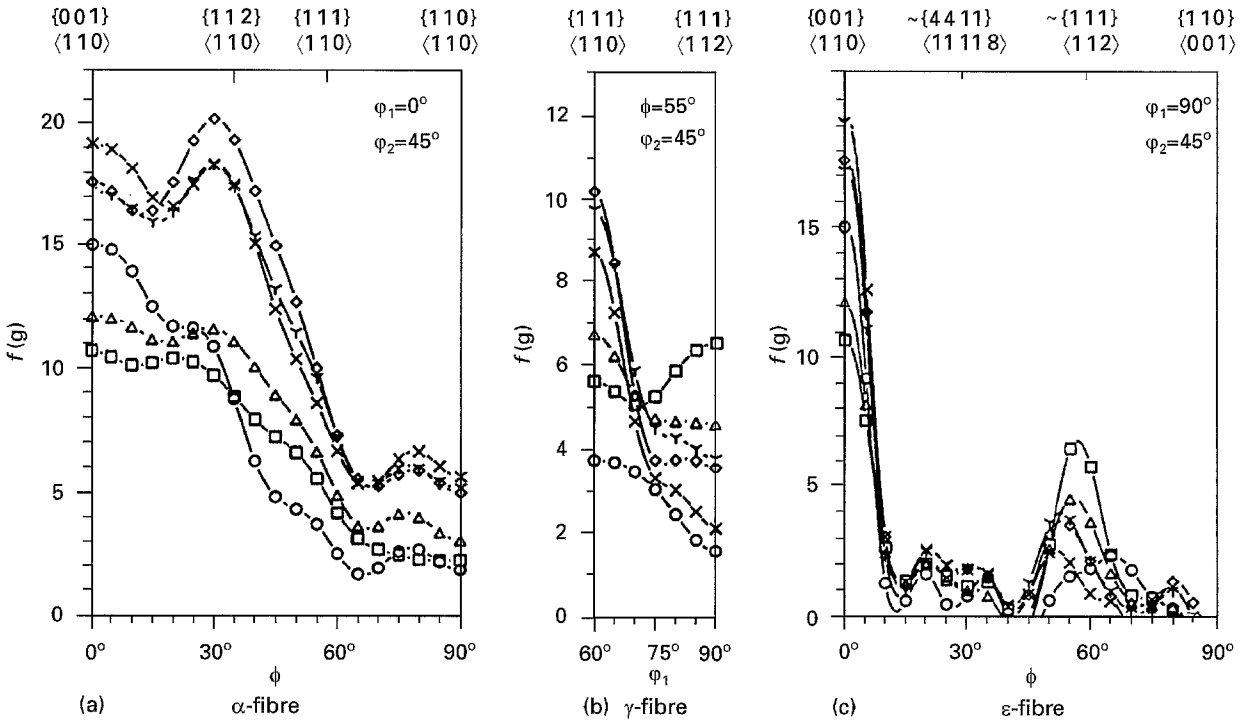

Figure 4 Hot and cold rolling texture of Fe–10.5 wt % Cr in fibre presentation, centre layer ($s = 0$) : (a) α-fibre, (b) γ-fibre, and (c) ε-fibre. Key: ○ hot band; □ 50%, △ 60%, × 70%; ⏜ 80%; ◇ 90%.

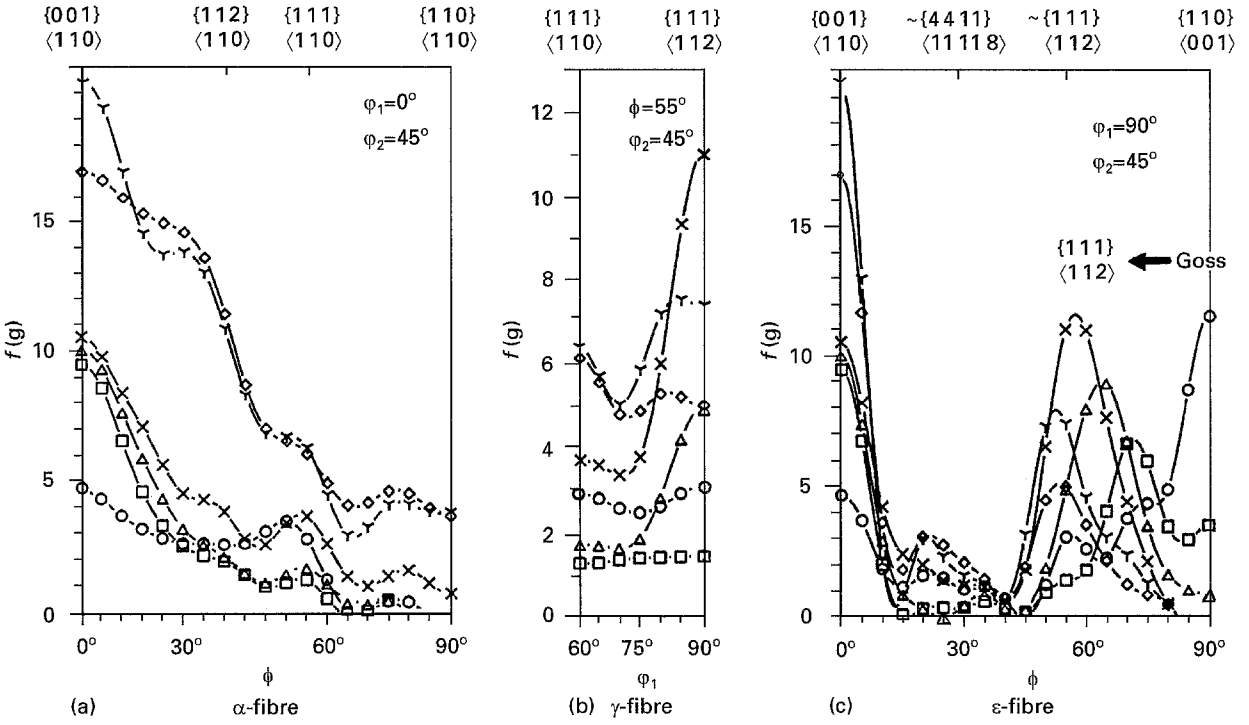

Figure 5 Hot and cold rolling texture of Fe–10.5 wt % Cr in fibre presentation, sub-surface layer ($s = 0.8$) : (a) α-fibre, (b) γ-fibre, and (c) ε-fibre. Key: ○ hot band; □ 50%; △ 60%; × 70%; ⏜ 80%; ◇ 90%.

very weak (Fig. 5a). With ongoing deformation the textures in both layers becomes somewhat more similar to each other. The results presented are also valid for other ferritic stainless steels with 10.5–16.5 wt % Cr content [5–14].

4. Discussion

4.1. Through-thickness inhomogeneity

As is evident from the data presented, in ferritic stainless steels a strong gradient of the texture is generated during hot rolling. The explanation of inhomogeneity

has thus to concentrate on hot rather than on cold rolling. The inhomogeneity of the shear strains was thoroughly examined by Sellars and co-workers [30–32]. In order to investigate the through-thickness profile of the strain state during hot rolling the distribution of the magnitude of equivalent strain, strain rate, Zener Holomon parameter and volume fraction recrystallized through the sheet thickness were thoroughly inspected and simulated by Beynon *et al.* [31] and McLaren and Sellars [30, 32]. The computation of the equivalent strains were carried out by employing an Eulerian finite element model. The simulations predicted a strong maximum of the equivalent strain at $s = 0.8$. Among various definitions used to compute the through-thickness profile of the equivalent strain, those which accounted either for the strain rates or for the accumulation of shear strains irrespective of their sign, yielded maximum shear strains at $s = 0.8$. This position corresponds to the commonly observed maximum of the Goss orientation in the hot band texture (Fig. 6). Similar predictions of the shear strain profile imposed during hot rolling of ferritic stainless steels were made by Fedoseev and co-workers [10, 18]. In their work the authors made use of an analytical method, namely, of the superposition of harmonic currents. Concerning the through-thickness course of the shear strains nearly identical results to those in [30–32] were achieved [10, 18]. Hence from both quantitative texture analysis and computer simulations it is suggested that the Goss component observed close to the surface after hot rolling is attributed to heavy shear deformation. The strong cold rolling texture observed in the centre layer is explained by the occurring plane strain deformation conditions there.

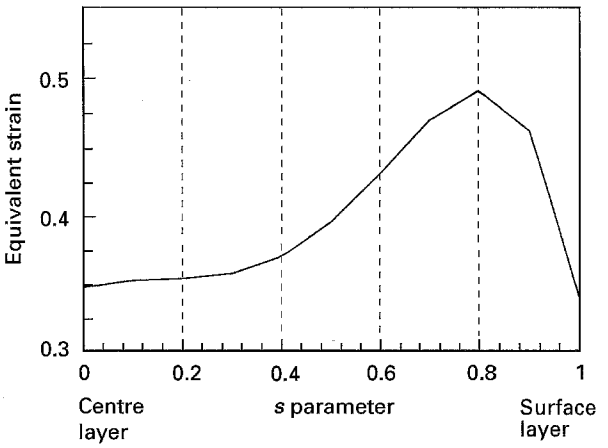

Figure 6 Through-thickness profile of the equivalent strain as computed by accumulating the shear strains irrespective of their sign [33]. The maximum of the shear strains occurs at $s = 0.8$. This position corresponds to the commonly observed maximum of the Goss orientation.

4.2. Influence of the Cr content

Hot rolling under industrial processing conditions was carried out by use of seven subsequent unidirectional rolling passes. Owing to their Cr (10.5–16.5 wt %) and C (0.01–0.02 wt %) content the steels under investigation undergo different amounts of

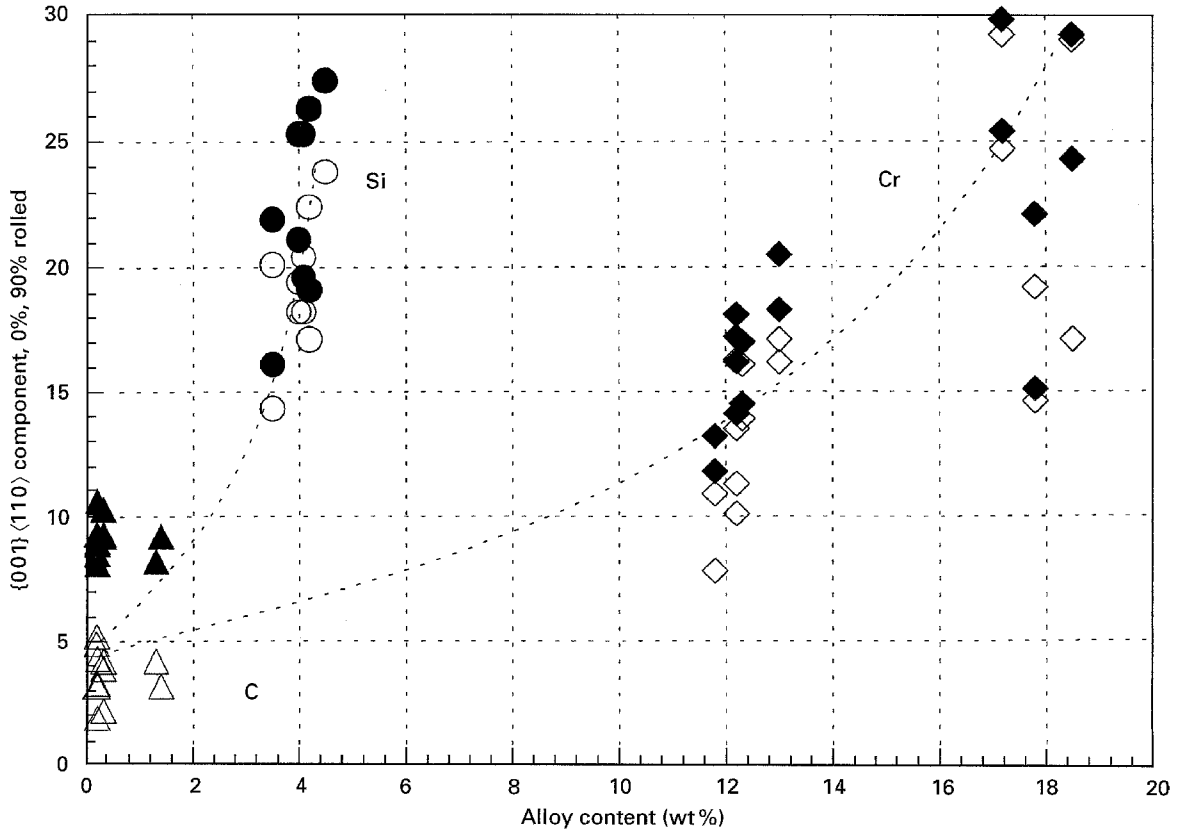

Figure 7 Orientation density of the {0 0 1} ⟨1 1 0⟩ texture component which usually dominates the rolling texture of Cr containing steels as a function of the total alloys content. Some results from Fe–Si and low-carbon steels were additionally considered.

phase transformation during industrial hot rolling [33, 34]. Whereas the first hot rolling pass is carried out within the temperature range, 1400 to 1460 K, the last one takes place within the range, 1200 to 1300 K. Since the C content is approximately the same for all alloys, steels which have a high Cr content are hot rolled mainly in the ferritic region and those with little Cr content more or less in the austenitic region.

From the texture results it is evident that during hot rolling a typical bcc cold-rolling type of texture [8] and close to the surface a typical bcc shear texture [9] is generated in the centre layers. Since both types of textures are very well known from other rolled bcc steels [14, 23–26] and bcc refractory metals [27, 28] it is strongly suggested by the current results that the texture formation has taken place essentially in the ferritic rather than in the austenitic region. Furthermore, it seems likely that the stronger the final hot band texture is the more hot-rolling passes have taken place in the ferritic region. This is also confirmed by hot band textures of low-carbon bcc steels which undergo nearly 100% phase transformation during cooling after hot rolling and hence show a nearly random hot band texture. In the present case, however, neither in alloys with little (10.5 wt %) nor in alloys with large (16.5 wt %) Cr content was this strong texture randomized by phase transformation or recrystallization [30].

Since the Cr content stabilizes the ferritic phase at elevated temperatures and reduces the austenitic region an attempt was made to relate the Cr content, which affects the transformational behaviour of the steels during hot rolling, to the resulting hot band textures. For this purpose the orientation density of the $\{0\,0\,1\}\langle 1\,1\,0\rangle$ texture component which usually dominates the rolling texture of Cr containing steels was, in a simplified approach, used as a measure for the type and sharpness of the resulting texture and thus plotted as a function of the total alloy content (Fig. 7). Additionally, some results from Fe–Si [29, 35] and low-carbon steels were considered [36, 37] (Fig. 7). From this presentation it becomes apparent that the increase of both Cr and Si, which have a stabilizing effect on the ferritic phase, lead to a stronger $\{0\,0\,1\}\langle 1\,1\,0\rangle$ component in the hot-rolled (open symbols) as well as in the 90% cold-rolled samples (full symbols). It is evident that the influence of Si exceeds even that of Cr. In order to examine this relationship between the texture and the thermodynamic behaviour of the steels during hot rolling more quantitatively, the volume fraction of the ferritic phase at 1270 K, which is within the temperature regime of the final hot rolling pass, was extracted from both experimental [38–41] and simulated [42] results (Fig. 8). Comparing Figs 7 and 8 substantiates that both the texture and the ferritic volume fraction at 1270 K reveal a satisfying correspondence. This result confirms the approach that the textures are essentially formed during the last hot rolling passes, i.e. in the ferritic region.

However, some deviations, especially for steels with 10.5 wt % Cr content, are also revealed. Although the thermodynamic data suggest a ferritic volume fraction not exceeding 33% for 1270 K and 10.5 wt % Cr [38–42] (Fig. 8), the orientation densities of the $\{0\,0\,1\}\langle 1\,1\,0\rangle$ component in the hot band textures of these steels (Fig. 7) shows merely somewhat lower values than the steels with 16.5 wt % Cr content. This

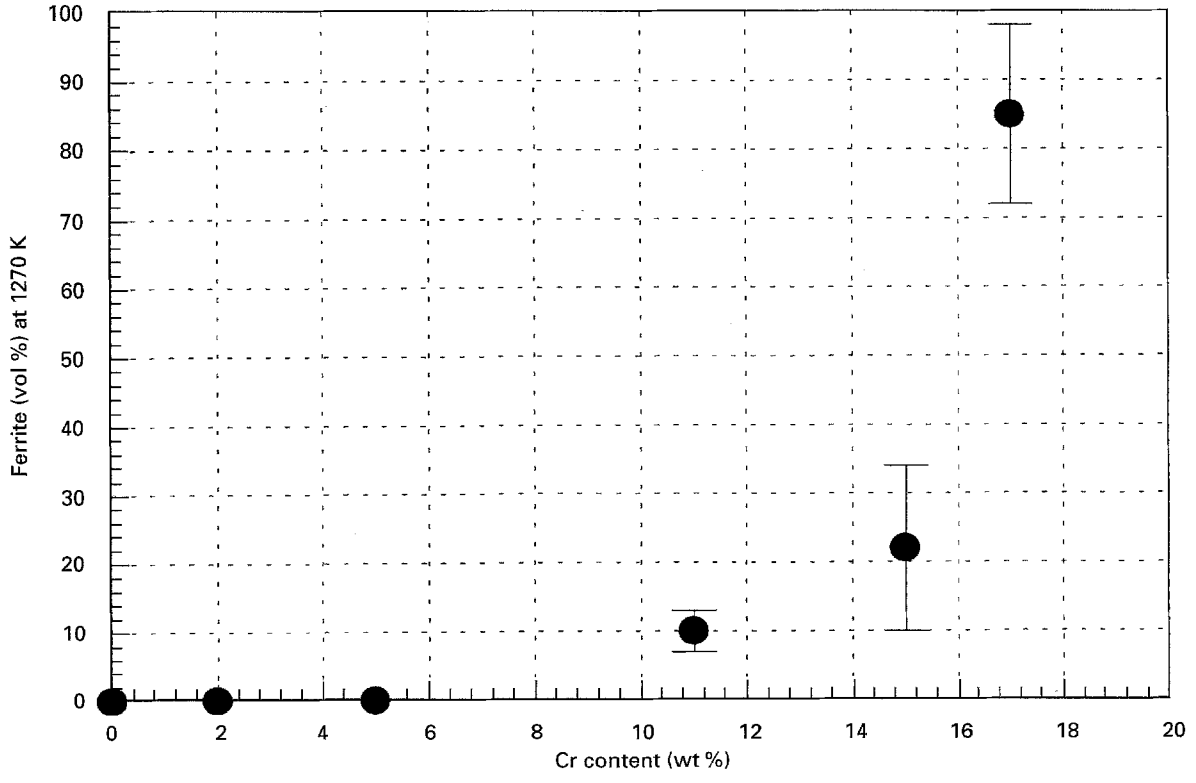

Figure 8 Volume fraction of ferrite in the last hot rolling pass (1270 K).

deviation is attributed to various causes. First, the impact of recrystallization and recovery was entirely neglected in the present comparison. Second, the complicated texture of the steels is represented by only one major component. Third, since only the Cr and the C content were considered for the estimation of the ferritic volume fractions the result was presumably not precise enough. Finally, the exact temperature at which the last hot rolling pass is carried out is not known very well. In the present estimation 1270 K was stipulated. Presumably, the real temperature is somewhat lower.

5. Conclusions

1. The textures of sixteen hot-rolled and cold-rolled stainless steels with 10.5–16.5 wt % Cr and 0.01–0.02 wt % C content were investigated. The hot band textures revealed a strong through-thickness texture inhomogeneity characterized by the occurrence of Goss at the surface ($s = 0.8$) and of the α-fibre in the centre layers.

2. Cold rolling led to an α-fibre texture in all layers. The strongest α-fibre occurred in the centre layers. Goss oriented grains at the surface ($s = 0.8$) rotated either towards $\{0\,0\,1\}\langle 1\,1\,0\rangle$ or $\{1\,1\,1\}\langle 1\,1\,2\rangle$.

3. Both the orientation densities of the $\{0\,0\,1\}\langle 1\,1\,0\rangle$ rolling component in hot-rolled and in 90% cold-rolled samples and the ferritic volume fractions at 1270 K were plotted as a function of the alloy content. The good agreement of both curves substantiated that the sharp rolling texture observed after hot rolling was formed in the ferritic region during the last hot rolling passes.

References

1. H. J. BUNGE, *Z. Metallkde* **56** (1965) 872.
2. *Idem*, "Texture Analysis in Materials Science" (Butterworths, London, 1982).
3. J. D. DEFILIPPI and H. C. CHAO, *Met. Trans.* **2** (1971) 3209.
4. R. M. DAVISON, *Met. Trans.* **6A** (1975) 2243.
5. M. HÖLSCHER, D. RAABE and K. LÜCKE, *Steel Res.* **62** (1991) 567.
6. D. RAABE and K. LÜCKE, *Scripta Metall.* **26** (1992) 1221.
7. *Idem*, in Proceedings of the 10th International Conference on Textures of Materials ICOTOM 10, Clausthal, September 1993, *Mater. Sci. Forum* **157–162** (1994) 597.
8. *Idem*, *Mater. Sci. Technol.* **91** (1993) 302.
9. M. HÖLSCHER, D. RAABE and K. LÜCKE, *Acta Metall.* **42** (1994) 879.
10. A. FEDOSSEEV and D. RAABE, *Scripta Metall.* **30** (1992) 1.
11. D. RAABE and K. LÜCKE, *Steel Res.* **63** (1992) 457.
12. D. RAABE, M. HÖLSCHER, M. DUBKE, H. PFEIFER, H. HANKE and K. LÜCKE, *ibid.* **64** (1993) 359.
13. D. RAABE and K. LÜCKE, in Proceedings of the International Conference on Strip Casting, Hot and Cold Working of Stainless Steels, Quebec, Canada, 1993, edited by N. D. Ryan, A. J. Brown, H. J. McQueen (The Metallurgical Society of CIM, Quebec, 1993) p. 3 and p. 221.
14. D. RAABE and K. LÜCKE, in Proceedings of the 10th International Conference on Textures of Materials ICOTOM 10, Clausthal, September 1993, *Mater. Sci. Forum* **157–162** (1994) 1469.
15. H. HONNEFF and H. MECKING, in Proceedings of the 6th International Conference on Textures of Materials ICOTOM 6, Japan, September 1981 edited by S. Nagashima (Iron and Steel Institute of Japan, 1981) p. 347.
16. U. F. KOCKS and H. CHANDRA, *Acta Metall.* **30** (1982) 695.
17. J. L. RAPHANEL and P. V. HOUTTE, *ibid.* **33** (1985) 1481.
18. A. FEDOSSEEV, D. RAABE and G. GOTTSTEIN, in Proceedings of the 10th International Conference on Textures of Materials ICOTOM 10, Clausthal, September 1993, *Mater. Sci. Forum* **157–162** (1994) 1771.
19. D. RAABE, *Mater. Sci. Technol.* in press.
20. M. HÖLSCHER, PhD thesis, Technical University of Aachen, Germany (1987).
21. D. RAABE, PhD thesis, Technical University of Aachen, Germany (1992).
22. L. G. SCHULZ, *J. Appl. Phys.* **20** (1949) 1030.
23. C. DÄRMANN, S. MISHRA and K. LÜCKE, *Acta Metall.* **32** (1984) 2185.
24. U. V. SCHLIPPENBACH, F. EMREN and K. LÜCKE, *ibid.* **34** (1986) 1289.
25. M. MATSUO, *ISIJ Int.* **29** (1989) 809.
26. W. HUTCHINSON, *Int. Mater. Rev.* **29** (1984) 25.
27. D. RAABE, G. SCHLENKERT, H. WEISSHAUPT and K. LÜCKE, *Mater. Sci. Technol.* **10** (1994) 229.
28. D. RAABE and K. LÜCKE, *Z. Metallkde* **85** (1994) 302.
29. L. SEIDEL, M. HÖLSCHER and K. LÜCKE, *Textures Microstruct.* **11** (1989) 171.
30. A. J. MCLAREN and C. M. SELLARS, in Proceedings of the International Conference on Strip Casting, Hot and Cold Working of Stainless Steels, Quebec, Canada, 1993, edited by N. D. Ryan, A. J. Brown, H. J. McQueen (The Metallurgical Society of CIM, Quebec, 1993) p. 107.
31. J. H. BEYNON, A. R. S. PONTER and C. M. SELLARS, in Proceeding of the Modelling of Metal Forming (Kluwer Acad. Publ., 1988) p. 321.
32. A. J. MCLAREN and C. M. SELLARS, *Mater. Sci. Technol.* **8** (1992) 1090.
33. E. HOUDREMONT, Handb. Sonderstahlkunde, 3. Aufl. (Springer Verlag **1**, 1956) p. 623.
34. K. BUNGARDT, E. KUNZE and E. HORN, *Arch. Eisenhüttenw.* **29** (1958) 193.
35. D. RAABE, Unpublished work.
36. C. KLINKENBERG, D. RAABE and K. LÜCKE, *Steel Res.* **63** (1992) 227.
37. Y.B. PARK, S. K. CHANG, D. RAABE and K. LÜCKE, *Mater. Sci. Forum* **157–162** (1994) 571.
38. O. KUBASCHEWSKI, "Binary Phase Diagrams of Iron" (Springer Verlag, Verlag Stahleisen m.b.H., 1982) p. 31.
39. E. SCHÜRMANN and J. BRAUCKMANN, *Arch. Eisenhüttenw.* **48** (1977) 3.
40. E. BAERLECKEN, W. A. FISCHER and K. LORENZ, *Stahl Eisen.* **81** (1961) 768.
41. H. ETTWIG and W. PEPPERHOFF, *Arch. Eisenhüttenw.* **41** (1970) 471.
42. G. KIRCHNER, T. NISHIZAWA and B. UHRENIUS, *Met. Trans.* **4** (1973) 167.

Received 19 October 1994
and accepted 13 February 1996